Validation of ITU-R P.833-9 tree attenuation model for Land Mobile Satellite propagation channel at Ku/Ka band

Sebastien Rougerie, Jonathan Israel, Kan Tomoshige

Validation of ITU-R P.833-9 tree attenuation model for Land Mobile Satellite propagation channel at Ku/Ka band

S. Rougerie[1], J. Israel[2], T. Kan[3]
[1]CNES, Toulouse, France, Sebastien.Rougerie@cnes.fr[1]
[2](ONERA): ONERA/DEMR, Université de Toulouse, France, jonathan.israel@onera.fr
[3]NICT, Tokyo, Japan, kan@nict.go.jp

***Abstract*— This paper presents a comparison between Rec. ITU-R P.833-9 ("slant path" section), versus measurements acquired by CNES and NICT at 20 and 18 GHz. Although several comparisons to measurements have been done between 1 and 3 GHz in previous works, we show here also a good agreement between Rec. ITU-R P.833-9 and the measurements at Ka band for satellite propagation channel, without excessive model tuning. The demonstration is done on isolated trees and long wooden road with an innovating fitting process.**

Index Terms*— *LMS, Ku/Ka band, ITU-R P.833, tree attenuation

I. INTRODUCTION

The effect of trees on propagation becomes all the more important when localization and communication systems are used extensively in static or nomadic applications. In L band, scattering effects due to tree trunks or branches can create significant code replicas which can impair GNSS system performances. In higher frequencies such as Ku or Ka bands, attenuation due to branches, needles or leaves lead to large scale fading undermining communication systems. Therefore, models have been developed in order to characterize trunks, branches, needles and leaves effects on propagation. The Multiple Scattering Theory (MST) introduced originally by Twerski [1] has been widely used in order to compute the scattering due to a tree canopy. Scatterers inside the canopy are described as dielectric cylinders for which approximations of the scattering behavior have been found [2] [3]. These works lead to the introduction of the section "slant path" in Recommendation ITU-R P.833-9 where for a given geometry (Tree shape and position, Rx and Tx positions) and a given canopy definition (branch size definition and density, see table 7 from ITU P.833-9) the specific attenuation of the tree canopy (dB/m) and the equivalent scattering cross-section per unit volume of the canopy can be estimated. Then, by integration, the recommendation provides the total attenuation, and the multipath scattered power relative to LOS. In order to ease its use in simulations in L to Ka bands, a point scattering model which reproduces the scattering behavior has been developed [4]. Point scatterers with specific parameters are sampled in any tree canopy volume and their contributions are computed based on the original Radar Cross Section (RCS) predicted by the Multiple Scattering Theory. Last, in [5], we have showed how these point scatterers contributions can be combined with trunk contributions and the attenuated components in order to perform electromagnetic simulations where the effect of a large set of trees is efficiently taken into account.

The comparison to measurements of the Multiple Scattering Theory (MST) and point scattering theory [4] [5] has been performed on several measurement campaigns in L-S and C band [6]. The purpose of this document is to present the model comparison to data at Ka band based on NICT and CNES measurement performed respectively at 18.9 GHz and 20 GHz. The document is organised as follow. Section 2 briefly presents the measurement campaigns and the selected area for model evaluation and section 3 compares the measurements with the point scattering model in the case of isolated tree. In Section 4, we propose to compare tree attenuation statistics between Recommendation ITU-R P.833-9 and time series measurement collected in wooden environment. A statistical validation is therefore done in section 4. Last, section 5 gives insight of some theoretical limitations of the point scattering model in order to apprise the user of the validation domain of the model, and finally, section 6 presents our conclusions.

II. MEASURMENTS CAMPAIGNS

A measurement campaign performed by NICT has collected satellite – mobile car communication RF data at 18.9 GHz. The measurement campaign and some results are presented in [7]. From this campaign, attenuation measurements behind trees were extracted as we can see in Figure 1 and Figure 2. Figure 3 presents the measured signal attenuation behind the tree for different seasons. We can see the attenuation may change as a function of the season until 10dB, certainly due to the presence or not of leaves.

In order to use these data for model comparison, additional information are necessary. From Figure 3, we can observe that the 2 observations (March 8th 2018 and April 12th 2018) are inside the power dynamic range.

Figure 1: NICT LMS tree measurements

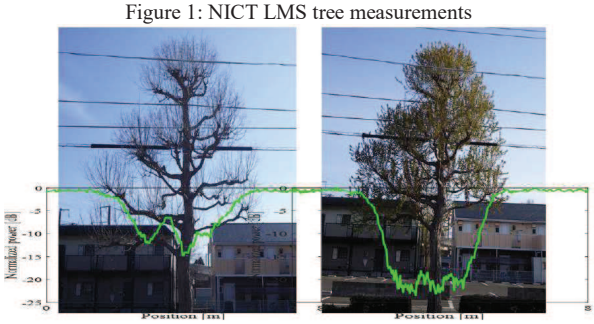

Figure 2: Signal attenuation behind Acer buergenianum tree for March 8th 2018 (left) and April 12th 2018

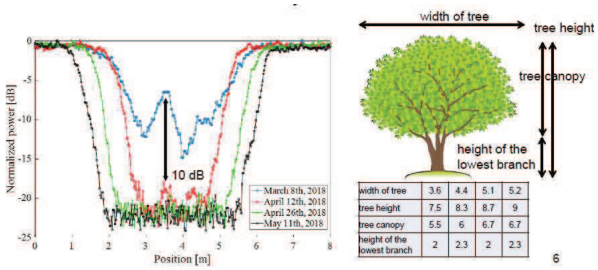

Figure 3: NICT measurement, signal attenuation behind Acer buergenianum tree for several season (left), tree dimension (right)

Indeed, we can estimate the noise floor around -22dB thanks to other measurements where this floor was reached (see April 26th and May 11th in Figure 3). Moreover, the shape of the tree has been measured, and we know the relative position between the tree and the car (Figure 1), as well as the elevation (40°). Thus, we have all the necessary information to reproduce this scenario in simulation (simulation for March and April) in order to compare measured and simulated time series.

CNES has performed similar measurements in France at 20GHz [10] [11] in several environments (urban, sub urban, highway, railway). From these measurements, we extracted a small trajectory where 3 similar trees were measured. Figure 4 presents the scenario where Rx trajectory, trees and LOS are represented. Here, the Rx is driving from the top right corner to the bottom left corner, and the LOS elevation and azimuth (angle from north to east) are respectively 28° and 133° (Rx and Tx position are known).

Figure 4: CNES LMS trees measurement

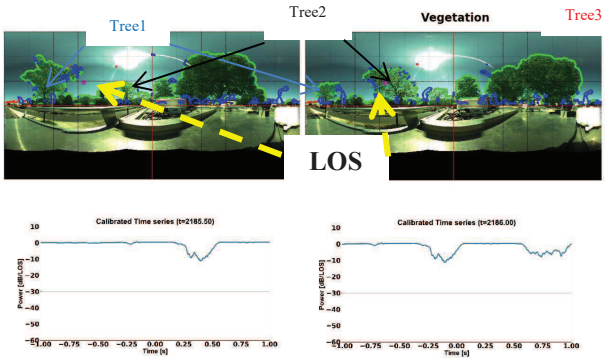

Figure 5: two 360° images, with vegetation detection

The 360° images concurrent to the RF data help to understand the geometry. The Figure 5 presents the images captured on this trajectory, where the trees were detected thanks to a "deep learning" algorithm. The centre of the image is the front of the vehicle, and the car is driven to the south west. Thus, the satellite position is on the left of the images (magenta point), same as the trees which obstruct the LOS.

Finally, the signal attenuation corresponding to those trees is plotted in Figure 5 and Figure 6. To reproduce this scenario in simulation, we need to know trees / Rx / Tx positions and trees shape. The Tx and Rx positions are perfectly known thanks to the satellite ephemerids and GPS receiver information. We approximatively estimate the tree positions thanks to Google Maps (Satellite view), and the shapes of the trees have been approximatively estimated to the following parameters: width = 3m, tree canopy = 3.5m and trunk height = 3.75m.

In order to have an easy and fast representation of the scenario, we assume the three trees have the same shape. Moreover, as is it the same tree specie, we assume similar stochastic parameters (see Table 2 in Section III).

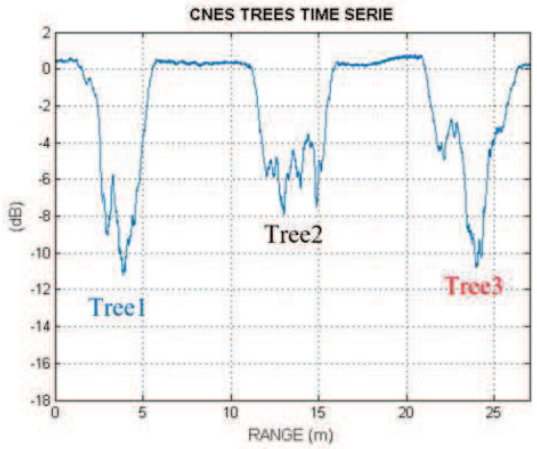

Figure 6: CNES measurement, signal attenuation behind the trees

Still from the CNES measurement campaign at 20GHz [10] [11], large wooded road were extracted. Indeed, the trajectory tagged as "Sub Urban" contains large portions of roads surrounded by trees (2 x 60 km [10]). From these trajectories, it was possible to extract only the tree attenuation statistics as we use 360° images processed by a deep learning algorithms in order to automatically detect when the signal is obstructed by trees [12]. Thus, tree attenuation statistical comparison between ITU-R P.833-9 model and experimental data will be tackled in section IV.

III. MODEL VALIDATION ON ISOLATED TREES

Both scenarii (NICT and CNES) have been reproduced in simulation by taking into account the geometry described in section II. The canopy and the trunk were modelled by cylinders.

However, other parameters must be defined. The first one is the antenna beam width. Unfortunately, this parameter is usually not given by antenna manufacturer for such "on the move" antennas. This parameter is important as it will impact the multipath power seen by the system. For NICT and CNES antenna, we assume here a 3° beam width.

The last parameters are the canopy definition (i.e. trees stochastic parameters). In Rec. ITU-R P.833-9, several categories of branches and one category of leaves are available as we can see in Table 1. In the case of both measurements, we remove the branches category 5 which corresponds to spine. Here, we tune only the branches density 4, and the leaves density (which can be equal to zero). An example of time series obtained with different values of branches (4) density is given in Figure 8. We can see that the higher the branches density, the higher the attenuation and the multipath contributions.

For the NICT measurements, there is only one tree to consider. Thus we optimize the stochastic parameters for this tree in order to fit as best as possible to the measurements. For the CNES measurements, there are three trees, but we assume similar stochastic parameters (same species). Thus, similarly to NICT, only two parameters are optimized to fit to the measurements.

Table 1 Size and density of branches and leaves available in ITU-R P.833-9 (TABLE 7)

Scatterer type	Radius (cm)	Length/thickness (cm)	Number density (m^{-3})
Branch (1)	11.4	131	0.013
Branch (2)	6.0	99	0.073
Branch (3)	2.8	82	0.41
Branch (4)	0.7	54	5.1
Branch (5)	0.2	12	56
Leaf	3.7	0.02	420

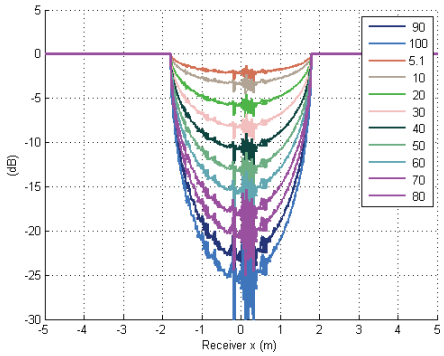

Figure 7: Attenuation time series for NICT, March Tree, with different values of branches (4) density (in m^{-3})

Table 2 describes the density values associated to the best fit. For the NICT tree, we use the same density branches (4) for March and April, and we just add leaves between both simulations. With a good leaves density, we can find the 10dB difference between both attenuation values, similarly to the observation Figure 8. We also find the trunk diffraction effect, with more energy when the satellite / car / tree are aligned. Thus, the simulation behavior and attenuation range are consistent with the observations.

However, we can observe that the multipath power is maybe too high. That can be compensated by using an antenna with a smaller beam width. With a more accurate antenna description, we may expect better results.

Regarding to the CNES measurements, similar behaviors are still respected (Figure 9). The simulated attenuations are in the same dynamic range as the measurements. The tree positions and shape are not perfect as there have been coarsely estimated (Google maps). Thus, the attenuations are not perfectly located in the time series. However, taking into account this very easy and fast reproduction of the scenario (same tree shape, same stochastic parameters), the predicted attenuation is still relevant, although the results may be improving by a better trees description. Here again, Table 2 summarized the optimized stochastic tree parameters for the CNES measurements.

Table 2: Branches (4) and leaves density associated to the best measurement fit

RF data	Branches (4) density (m^{-3})	Leaves density (m^{-3})
NICT, March 2018	50	0
NICT, April 2018	50	200
CNES	50	30

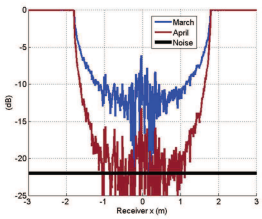

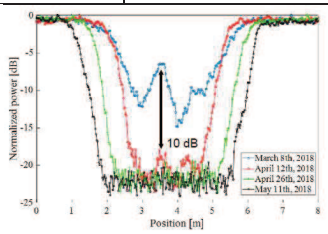

Figure 8: NICT tree, simulated time series (left) vs measured time series (right)

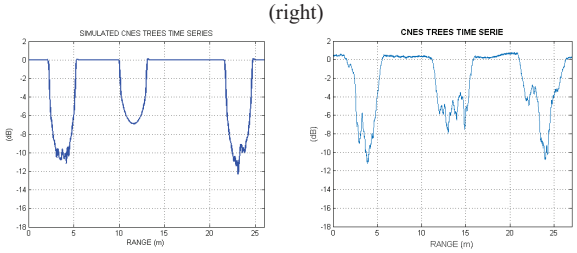

Figure 9: CNES trees, simulated time series (left) vs measured time series (right)

IV. MODEL VALIDATION ON LARGE WOODED ROAD

The total attenuation due to the propagation through a tree observed by a receiver will depend on the tree canopy size. In section 3, those sizes were known and introduced in the simulator. Here, we tackle the case of long time series, and it is necessary to have first an estimation of the canopy size statistic along this trajectory. We propose in this section a simple geometry model Figure 10, and the total attenuation is thus given by:

$$Att(x) = 2Att_{lineic}R\sqrt{1-\left(\frac{x}{R}\right)^2} \quad (1)$$

With Att_{lineic} the linear attenuation given by Rec. ITU-R P.833-9, R the radius of the canopy, and x the relative positon in the tree frame.

Based on a deep learning processing on concurrent 360° images to the RF signal, we can extract from the measurement an attenuation statistic due only to the tree. Thus, we can measure the statistics of the *Z(x)* random variable defined as:

$$Z(x) = \frac{Att(x)}{2Att_{lineic}} = R\sqrt{1-\left(\frac{x}{R}\right)^2} \quad (2)$$

The challenge is now to estimate the distribution of R based on the distribution of Z. The first step is to introduce the random variable Z' with $g_{Z'}(x) = \frac{g_Z(x)}{x}$ ($g_\xi(x)$ denotes the density function of ξ). Z' follows the same distribution of Z, and can be generated thanks to independent random process:

$$Z' = R\sqrt{1-Y} \quad (3)$$

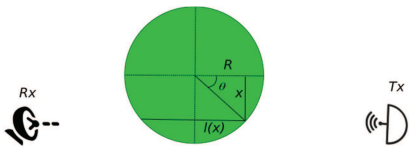

Figure 10: Propagation through the canopy

With Y a new random process independent of R which must follow (4).

$$g_y(k) = \int_k^1 g_y(x)dx \quad (4)$$

The cumulative distribution function, denoted as $F_\xi(x)$, (4) becomes:

$$F_y(2k-k^2) = k \quad (5)$$

The cumulative distribution of $R = Z'W$ with $W = \frac{1}{\sqrt{1-Y^2}}$ can be therefore estimated by:

$$F_R(a) = \int_0^k F_{Z'}\left(\frac{a}{x}\right) g_W(x)dx \quad (6)$$

Based on this regression technic, it was possible to extract the distribution of R, and we introduce this distribution in the random 3D scenario in the Ku/Ka simulator which includes Rec. ITU-R P.833-9 [12]. Tree positions were assumed along a straight road with a range of several kms. Finally, the statistics comparison is done Figure 11, and shows a good agreement between the simulations and the measurement.

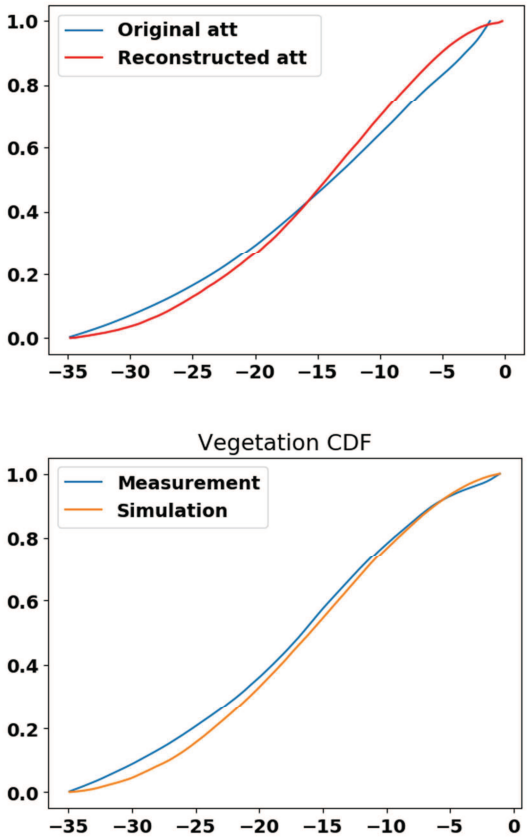

Figure 11: Comparison trees attenuation statistics between CNES measurement and ONERA/CNES simulator which includes ITU-R P.833-9 recommendation. Top comparison on whole trajectory, bottom comparison on vegetation only

V. ITU-R P.833-9 MODEL DISCUSSION

In this section, we discuss about the limitation of the model. Two assumptions are necessary if we want to use correctly the model: one at low frequency, and another on at high frequency. The far field assumption is needed in the MTS [1] [2] [3]. The receiver must be therefore far enough from the scatterers, and we have to respect $\frac{2\pi}{\lambda}x \gg 1$ with λ the wavelength, and x the range between the Rx and scatterers. This limitation mostly impacts low frequencies: for F = 1 GHz (L band), the range must be higher than 5cm, which is acceptable. For F = 30 GHz, x>>1.5mm which is definitively not a problem. The MST assumes no multiple interaction between the scatterers or in other word, each scatterers are enough spaced inside the canopy. The equation to respect is $y \gg \frac{d^2}{2\lambda}$, with d the size of the scatterers (i.e. branches or leaves), and y the range between 2 scatterers. This limitation mostly impacts high frequencies. For example, for a 30cm branches size and F = 30 GHz, we must have y > 4.5m. Here appears the main limitation for high frequencies. The main consequence is that the multipath component may be overestimated. In Figure 12, we plot time series for several antenna beam widths. Higher is the antenna beam width, higher is the multipath contribution, and we can see the MP power may overcome the LOS power which is physically impossible.

A trick to limit the multipath power is to use very narrow beam width, and this is the case for satellite communications at high frequencies. For example, according to the ITU recommendation [8]-[9], the antennas of an earth station operating with a geostationary satellite should have a design objective where the main-lobe axis φ_{min} must not exceed 3°. With such antenna design, the multipath diffusion is strongly limited, and the results look coherent with the observation as we demonstrate in sections III and IV.

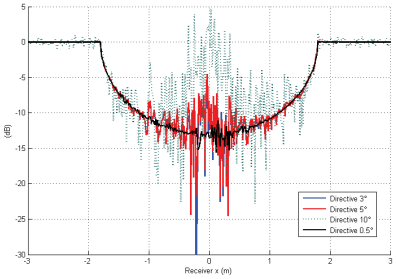

Figure 12: Times series for NICT tree March, with different antenna beamwidth

VI. CONCLUSIONS

If the comparison to measurements of the Multiple Scattering Theory (MST) (i.e. theoretical base of the ITU-R P.833) [4] [5] [6] has been performed at L-S and C band [6], here we propose new comparison elements at Ka band for isolated trees and wooden road thanks to measurement done by NICT and CNES at 18 and 20 GHz.

In the case of isolated tree validation, all the geometrical elements have been defined with a deterministic approach (Rx, Tx, Tree positions, Tree shape), and we assumed 3° antenna beam width in accordance to the ITU antenna recommendation [8] [9]. The stochastic parameters of the ITU-R P.833-9 were tuned in order to be representative of several trees species, and canopy evolution as a function of the seasons. From the recommendation, we do not change the branches and leaves size, but only modify one category of branches density and the leaves density inside the canopy. By tuning only these two elements, we have been able to reproduce the attenuation observed behind each trees, whatever the species and the season.

In the case of long times series associated to long wooden road, here again the recommendation ITU-R P.833-9 provide very reliable results, but statistics of the canopy size must be estimated before.

Last but not least, this paper presents in the last section the main limitation of the ITU-R P.833-9. For high frequencies (above 10 GHz), the user should be aware that the multipath contribution can be overestimated in the case of antenna with a very large beam width. Fortunately for space applications, the link budget at such high frequencies require antennas with important gains and thus, very directive beams. Finally, the recommendation is still reliable for high frequencies by taking into account this system constraint.

REFERENCES

[1] V. Twersky, “Multiple scattering of electromagnetic waves by arbitraconfigurations,” Journal of Mathematical Physics, vol. 8, p. 589, 1967.

[2] M. Karam, A. Fung, and Y. Antar, “Electromagnetic wave scatteringR-REP-P.2097.2007 from some vegetation samples,” IEEE Transactions on Geoscience and Remote Sensing, vol. 26, no. 6, pp. 799 –808, Nov. 1988

[3] M. Karam and A. Fung, “Leaf-shape effects in electromagnetic wave scattering from vegetation,” IEEE Transactions on Geoscience and Remote Sensing, vol. 27, no. 6, pp. 687–697, 1989.

[4] J. Israel, F. Lacoste, H. J. Mametsa, and F. P. Fontan, “A propagation model for trees based on multiple scattering theory,” in Antennas and Propagation (EuCAP), 2014 8th European Conference on, April 2014, pp. 1255–1258

[5] J. Israel, A. Pajot “Fading and scattering due to trees in L to Ka band propagation simulationsA propagation model for trees based on multiple scattering theory,” in Antennas and Propagation (EuCAP), 2015 9th European Conference on

[6] G. Carrié, F.Perez Fontan, F.Lacoste, J.Lemorton, “A Generative MIMO Channel Model Encompassing Single Satellite and Satellite Divesity cases ». ESA workshop on radiowave propagation, Noordwijk, NL, November 2011

[7] T. Kan, B. Jeong, H. Susukita, K. Kawasaki, T. Takahashi and M. Toyoshima, “Experimental Results of Seasonal Variation of Shadowing by Ka-band Mobile Satellite Communication”, 32nd International Symposium on Space Technology and Science (ISTS), 2019-j-11, June 2019

[8] http://www.itu.int/rec/R-REC-S.580/en

[9] http://www.itu.int/rec/R-REC-S.465/en

[10] S. Rougerie, B. Benammar, Concurent Ka band RF measurement and Fish-eye Images for Land Mobile Satellite Propagation Channel, EuCAP 2018, London

[11] S. Rougerie, J. Israel, Mobile Satellite Propagation Channels at Ka band for railway and highway environement, EuCAP 2019

[12] J. Israel, S. Rougerie, A Physical – Statistical hybrid model for land mobile satellite propagation channel at Ku/Ka band, EUCAP 2020